Accepted Manuscript

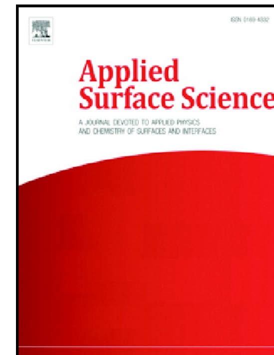

2D compositional self-patterning in magnetron sputtered thin films

Aurelio García-Valenzuela, Rafael Alvarez, Victor Rico, Juan P. Espinos, Maria C. López-Santos, Javier Solís, Jan Siegel, Adolfo del Campo, Alberto Palmero, Agustín R. González-Elipe

PII: S0169-4332(19)30557-4
DOI: https://doi.org/10.1016/j.apsusc.2019.02.206
Reference: APSUSC 41901

To appear in: *Applied Surface Science*

Received date: 11 October 2018
Revised date: 13 February 2019
Accepted date: 23 February 2019

Please cite this article as: A. García-Valenzuela, R. Alvarez, V. Rico, et al., 2D compositional self-patterning in magnetron sputtered thin films, Applied Surface Science, https://doi.org/10.1016/j.apsusc.2019.02.206

This is a PDF file of an unedited manuscript that has been accepted for publication. As a service to our customers we are providing this early version of the manuscript. The manuscript will undergo copyediting, typesetting, and review of the resulting proof before it is published in its final form. Please note that during the production process errors may be discovered which could affect the content, and all legal disclaimers that apply to the journal pertain.

ACCEPTED MANUSCRIPT

2D compositional self-patterning in magnetron sputtered thin films

Aurelio García-Valenzuela,[1] Rafael Alvarez,[1,2] Victor Rico,[1] Juan P. Espinos,[1] Maria C. López-Santos,[1] Javier Solís,[3] Jan Siegel,[3] Adolfo del Campo,[4] Alberto Palmero,[1] Agustín R. González-Elipe[1*]*

1.- Nanotechnology on Surfaces Laboratory. Instituto de Ciencia de Materiales de Sevilla (CSIC-Univ. Sevilla). Avda. Américo Vespucio 49. 41092 Sevilla

2.- Departamento de Física Aplicada I. Escuela Politécnica Superior, Universidad de Sevilla. c/ Virgen de África 7, 41011, Seville, Spain

3.- Laser Processing Group. Instituto de Optica (CSIC). c/Serrano 117. Madrid (Spain)

4.- Departamento de Electrocerámica, Instituto de Cerámica y Vidrio (ICV-CSIC), C/Kelsen 5, 28049 Madrid, Spain

*e-mail: arge@icmse.csic.es; aurelio.garcia@icmse.csic.es

Keywords: thin film composition, patterning, magnetron sputtering, SiOx, LIPPS

Abstract

Unlike topography patterning, widely used for numerous applications and produced by means of different technologies, there are no simple procedures to achieve surface compositional patterning at nanometric scales. In this work we have developed a simple method for 2D patterning the composition of thin films. The method relies on the magnetron sputtering deposition at oblique angles onto patterned substrates made by laser induced periodic surface structures (LIPSS). The method feasibility has been demonstrated by depositing SiOx thin films onto LIPSS structures generated in Cr layers. A heterogeneous and aligned distribution of O/Si ratios (and different Si^{n+} chemical states) along the LIPSS structure in length scales of some hundreds nm´s has been proven by angle resolved X-ray photoelectron spectroscopy and a patterned arrangement of composition monitored by atomic force microscopy-Raman analysis. The obtained results are explained by the predictions of a Monte Carlo simulation of this deposition process and open the way for the tailored one-step fabrication of surface devices with patterned compositions.

ACCEPTED MANUSCRIPT

Keywords: compositional patterning, LIPPS, surface composition, angle resolved XPS, magnetron sputtering, SiOx thin films

Introduction

Topographic pattering using optical lithography [1,2], ion or electron beam bombardment [3,4] or laser treatment [5], among other methods, are common procedures for the surface processing of a large variety of materials. However, no equivalent techniques exist for patterning the surface composition in scale ranges in the order of hundreds of nanometers, a possibility that would open new interesting pathways in applications areas such as wetting and freezing, photonics or advanced electronic devices [6-8]. The herein proposed procedure for surface composition patterning in a hundred nanometer scale relies on the deposition of thin films by magnetron sputtering at oblique angles (MS-OAD) [9] onto a substrate patterned with Laser-Induced Periodic Surface Structuring (LIPSS)[10, 11]. Equivalent results would be obtained onto similar surfaces covered by linear grooves prepared by other methods.

A well-established feature of OAD thin films when prepared onto flat substrates, either by electron beam evaporation or MS, is the formation of a porous microstructure in the form of tilted nanocolumns [12]. On patterned substrates, electron beam evaporation in this geometrical configuration has been used for the fabrication of sculptured thin films, multilayers or other type of well-ordered surface nanostructures [13,14]. Generally and independently of the complexity of the microstructure and surface topography of the obtained thin films, composition remains invariable in these deposition processes, both laterally and in depth.

In a very recent work using reactive magnetron sputtering (r-MS) deposition at oblique angles (r-MS-OAD) [15], we have reported that the tilting angle of nanocolumns and the composition of SiOx thin films (i.e., the value of x, ranging from 0.4 to 2.0) can be effectively controlled by adjusting the deposition angle and the partial pressure of oxygen in the plasma gas. Relying on this methodology, in the present work, SiOx thin films with well-defined x values (as determined on flat substrates) have been deposited onto a substrate consisting of ca. 800 nm separated lineal patterns produced by Laser-Induced Periodic Surface Structures (LIPSS) onto a metal film [16,17]. An analysis of the angular dependence of the Si2p X-ray

ACCEPTED MANUSCRIPT

photoelectron spectra (i.e., angle resolved XPS [18,19]) has shown that the local composition of the deposited layers self-adjusts along the ripple structure (i.e., there is a self-modulation of the surface composition). Moreover, 2D maps recorded with AFM-Raman [20] confirmed that surface composition varies in a periodic way following the sequence defined by the topographic rippled structure of the substrate. Finally, to understand the basis of the shadowing effects controlling this surface modulation of composition, we have simulated the deposition process by a Monte Carlo model [21,22] that takes into account the trajectories and local impingement angles of the sputtered silicon atoms onto the different zones of the ripple substrate. The good agreement between simulations and experiments support the general character of the method and its potential use with other thin film materials (e.g., nitrides, mixed oxides, etc.) and substrates.

Experimental and Methods

The substrates used for oblique angle deposition were nanostructured by fs-laser irradiation as described in ref. [16]. They consisted of 1 µm thick Cr films, evaporated onto a multilayer substrate made of a top Ni layer (20 µm thick), an intermediate adhesion layer made of Cu (1 µm thick), and a 1 mm thick polymer slab. The samples were irradiated using a fiber-based fs-laser amplifier (Tangerine, Amplitude Systems) emitting ~ 450 fs laser pulses at 1030 nm at a repetition rate of 250 kHz. The samples were irradiated with the fundamental wavelength of the laser (1030 nm). Beam energy was controlled by means of a lambda-half ($\lambda/2$) wave plate/thin film polarizer system. After energy control, the beam passes through a second $\lambda/2$ wave plate for polarization control. The beam is then sent through a galvanometer scanning unit equipped with an F-Theta lens (100 mm focal length) to scan the focused beam over the static sample. The scanning speed used was 1500 mm/s and the pulse energies were typically in the range of 0.5-2 µJ/pulse. In all cases, the beam polarization was set perpendicular to the beam scanning direction in order to promote the coherent propagation of LIPSS over large areas as shown in refs. [16,17] for 1030 nm radiation.

Deposition of SiOx thin films was carried out as described in ref 15 and schematized in Figure 1. Substrates were azimuthally oriented in such a way that the groove

ACCEPTED MANUSCRIPT

direction was perpendicular to the particle trajectory from the target to the substrate. Tilting angle of the substrate plane with respect to the upper sputtering track of the target was adjusted to an angle of 85º. The magnetron was operated in pulsed DC mode at a power of 200 W and a Ar flow of 6.25 sccm (working pressure of $1.5x10^{-3}$ mbar). Addition of oxygen to the plasma gas was used to control the O/Si ratio. This was determined by Rutherford Back Scattering (RBS) analysis of a thin film deposited on a nearby flat substrate of graphite. This O/Si ratio determined on flat substrates has been taken for sample designation. Several experiments were carried out with SiOx thin films with compositions defined by x= 1.2, 1.5 and 1.9, that were obtained by controlling the oxygen flow in the plasma gas (i.e., 0.78, 0.96 and 1.15 sccm, respectively). On flat silicon substrates, the equivalent thickness of the deposited SiOx thin films as determined by SEM was in the order of 45 nm.

X-ray photoelectron spectroscopy (XPS) analysis of the deposited thin films was carried out in a PHOIBOS spectrometer working in the pass energy constant mode fixed at 30 eV. Binding energy (BE) scale was referred to the C1S peak of the adventitious carbon contaminating the surface of samples taken at a value of 284.5 eV. Spectra were recorded by setting the exit angle of photoelectrons at normal and grazing exit directions (i.e., in angle resolved XPS mode [18,19]). To do that, samples were turned by the selected angles with respect to the energy analyzer entrance. Si 2p spectra were fitted under the assumption of a distribution of Si^{0}, Si^{+}, Si^{2+}, Si^{3+} and Si^{4+} oxidation states separated by approximately 1 eV in BE. This assumption is well documented in the literature [23-25] and has been successfully used for the fitting analysis of the Si2p peaks recorded in the present work.

Atomic Force Microscopy (AFM) analysis of the surface topography of LIPPS samples before and after SiOx thin film deposition has been carried out in a Nanotec AFM microscope supplied with a Dulcinea electronics.

Top view scanning electron microscopy (SEM) images were acquired with a field emission microscope (FESEM model Hitachi S4800 at the Instituto de Ciencia de Materiales de Sevilla, CSIC-US, Seville, Spain).

AFM-Raman analysis of the samples was carried out in a Witec Alpha-300RA (Ulm, Germany) confocal Raman microscope. A Nd:YAG laser of 532 nm wavelength was used to record the Raman spectra and Raman images. Raman maps of the sample surfaces whit an area of 7,5×7,5 µm were taken point by point with a piezo-driven

ACCEPTED MANUSCRIPT

stage and an optical fiber of 50 μm in diameter as pinhole to guarantee a spatial resolution less than 300 nm, through a 100X objective lens and numerical aperture of 0.95. Raman images were created by 50x50 full spectra (from -100 to 1100 cm^{-1}) (2500 specta), at 2 mW incident laser power, an acquisition time of 1 second per spectrum, requiring 50 min for each Raman map. Finally, the collected data were analyzed by using Witec Control Plus Software. An AFM coupled to the Witec Alpha-300RA confocal Raman microscope was used to obtain the topographic information of the samples. AFM images were taken in non-contact mode and using a NSG30 gold-coated silicon cantilever (with a resonant frequency of 268 kHz) supplied by NT-MDT (Moscow, Russia) whit a tip of 10 nm of radius and 15 μm of height. Under these conditions, AFM images were captured by scanning 256 lines with 256 points per line. The selected areas (10×10 μm) were those previously studied by Raman images.

Simulation of the thin film growth on the patterned substrates was performed using a well-tested Monte Carlo model to describe the MS-AOD of thin films. Main features of this model has been discussed in detail in previous works [21, 22]. This model assumes the incorporation of vapor species on a substrate according to certain angular distribution of arrival, filling in a three dimensional $N_L \times N_L \times N_H$ grid, whose cells may take the value 0 (empty) or 1 (full). In our case, each cell represents a Si species in the film that may be oxidized during deposition by reaction with the gaseous oxygen species impinging onto the surface. In the present work, this model has been applied to describe the deposition of SiOx thin films on an ideal sinusoidal rippled substrate characterized by amplitude and period of 160 And 800 nm, respectively.

ACCEPTED MANUSCRIPT

ACCEPTED MANUSCRIPT

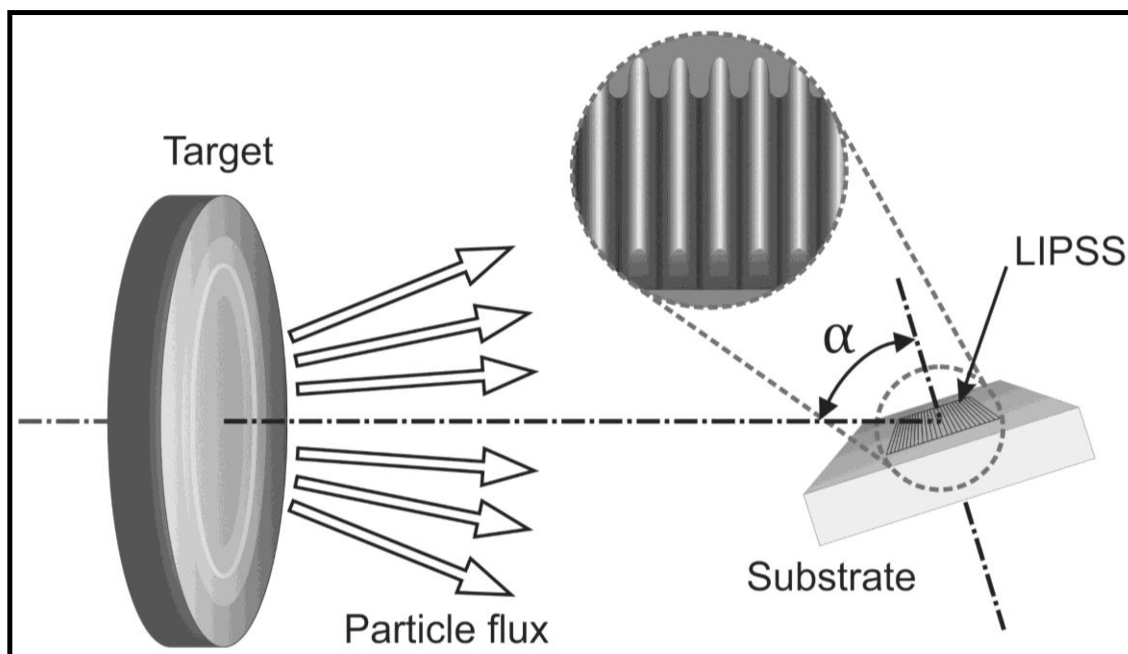

Figure 1.- Scheme of the geometrical arrangement of the rippled substrate with respect to the sputtering target during SiOx deposition. Substrate perpendicular forms 85º with respect to the sputtering target.

Results and discussion

r-MS-OAD of SiOx thin films onto linear patterned substrates

The patterned substrates used in the present work consist of a series of parallel and lineal grooves with an amplitude of approximately 250 nm and a period of 700 nm. SEM and AFM images of these substrates are reported in Figure 2 top. The morphology of these rippled substrates after SiOx deposition at 85º was also examined by SEM and AFM (Figure 2 bottom). The comparison of the images before and after deposition clearly shows that although a SiOx layer of approximately 45 nm has been deposited onto the rippled structure, the sinusoidal surface topography is still preserved, even if some blurring and broadening of the ripple pattern has occurred after the accumulation of deposited material. The groove amplitude (see the cross sectional lineal profiles in the middle panels of the figure) slightly changed as resulting from a partial filling of valleys by the deposited material (note that estimation of valley depth may be underestimated due to the finite size of the AFM tip).

ACCEPTED MANUSCRIPT

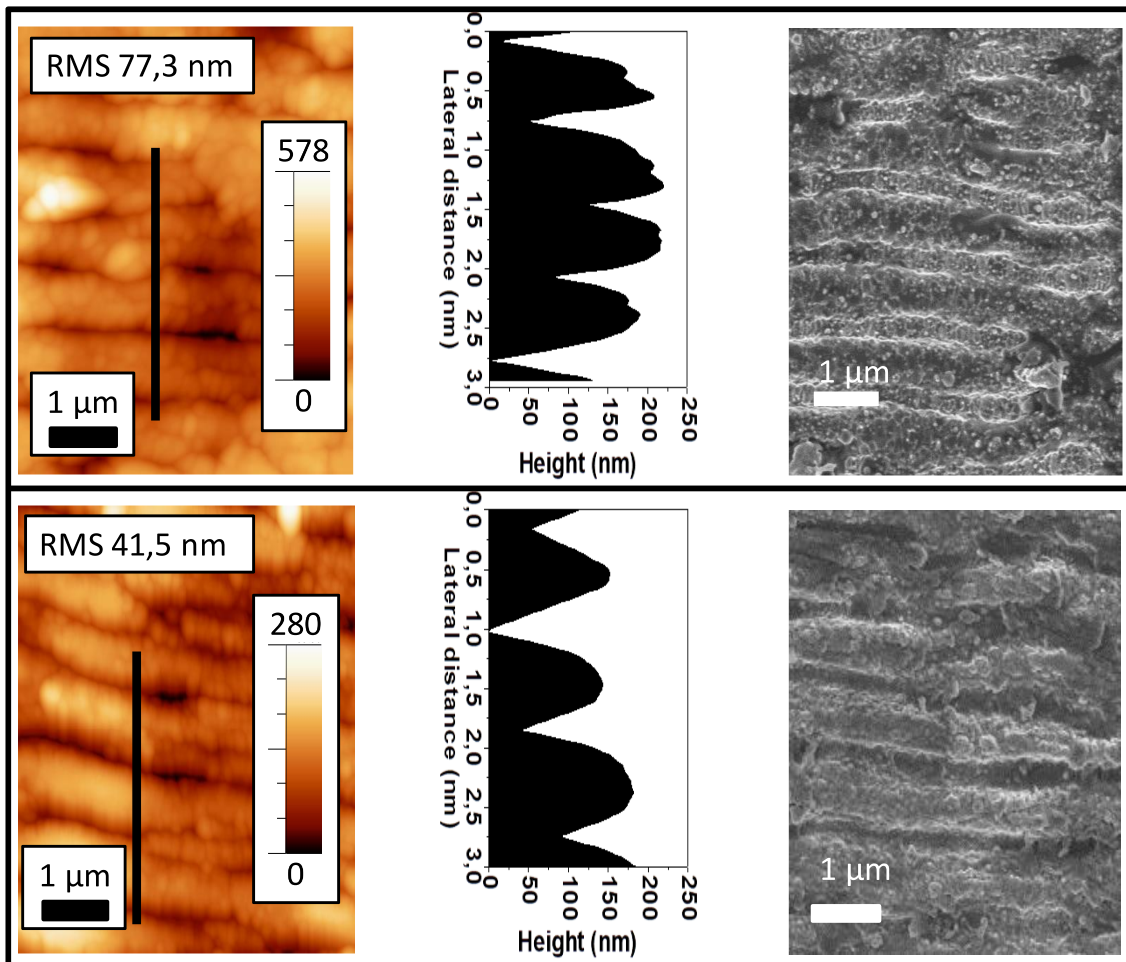

***Figure 2**.- Top) AFM (left) and SERM (right) images of the ripple substrates utilized for the deposition of the SiOx films before (top) and after (bottom) the MS-OAD of a $SiO_{1.5}$ thin film with a nominal thickness of 45 nm as determined on a nearby flat silicon substrate. Topography cross section lineal profiles are shown in the centre of the images (note the differences in the scales).*

MC simulation of deposition process

During MS-OAD the particle trajectories of a part of sputtered silicon species is affected by scattering events with the plasma gas and particles become thermalized before arriving to the substrate surface (see the scheme in Figure 3a) [9,15, 21, 22]. This phenomenon is well-known in magnetron sputtering depositions and is associated to the different collisional transport of sputtered species from the target to the film. In general, three type of species can be differentiated attending to their momentum distribution: i) ballistic species, i.e., particles that do not experience any collision in the gas phase and arrive at the film with their original momentum, ii)

ACCEPTED MANUSCRIPT

thermalized species, i.e., particles that undergo enough elastic scatterings in the gas phase to possess an isotropic momentum distribution when deposited, and iii) partially thermalized species, i.e., particles that, although have experienced several collisions, do not have a completely isotropic momentum distribution [26]. In previous works we have analyzed the degree of thermalization as a function of the plasma gas pressure and the distance between target and substrate [9]. For the conditions of the present experiment (i.e., with the substrate at a deposition angle of 85º and considering the total pressure and the distance between target and substrate), it can be estimated that approximately 45 % of the silicon particles were thermalized before arriving to the patterned substrate surface.

Under these conditions, the MC simulation of the deposition process reported in Figure 3b) shows that the film does not only grow in the region of the ripples facing the sputter target, but also at their back side. In this way, while the deposition of Si in the region of the ripples facing the target combines the three regimes of silicon species, at the back side of the ripples, only those that are thermalized or partially thermalized are allowed to be deposited. This explains the different growth rates on both sides of the ripples, as well as the different nanostructures predicted by MC simulation (Figure 3b)): while the region facing the target is rather compact due to a relatively high ballistic component, that at the back side of the ripples resembles vertically aligned porous structures, typical of a film grown by isotropically directed deposition species [27]. Since the oxygen impingement rate over the whole surface should be the same, and considering an adsorption probability independent of the film stoichiometry (an approximation that was already checked in ref. [15]), we also estimated the chemical composition on different parts of the film surface as a function of the relative Si and oxygen impingement rates on each side. The result of these calculations is represented by different colors in Figure 3c). In the region facing the target, the higher deposition rate of Si species leads to the formation of a sub-oxide layer ($x<2$), whose thickness decreases near the top of the ripple and at its back. On the back side a full stoichiometric oxide composition (i.e. SiO_2) would be obtained by assuming that the oxygen impingement rate is equivalent to that of silicon species and therefore enough to fully oxidize the deposited layer. It is also predicted that the local stoichiometry parameter x´ of the film on the side facing the

ACCEPTED MANUSCRIPT

target (i.e. $SiO_{x'}$) is smaller than the average x parameter of the film deposited onto a flat substrate (i.e., SiO_x).

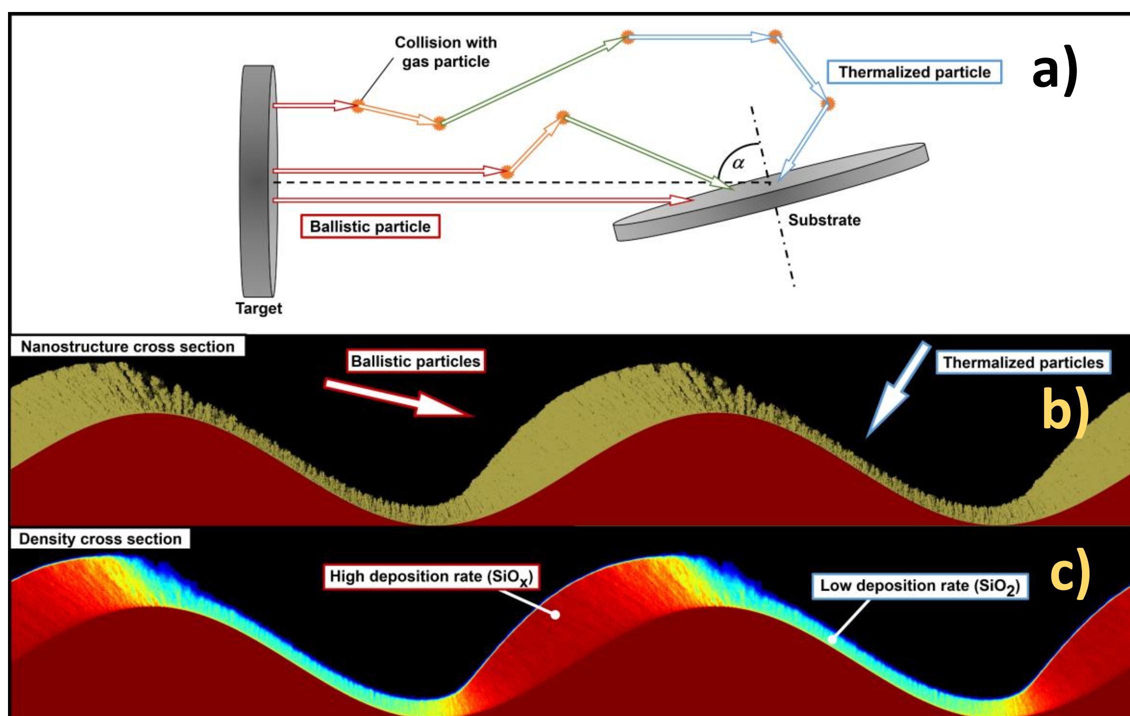

***Figure 3**. MC calculation of the SiOx deposition at an oblique angle of 85º onto an ideal sinusoidal substrate for an equivalent film thickness of 70 nm on a flat substrate. a) Scheme describing the partial thermalization process of particles in their trajectory from the target to the substrate. b) Simulated cross section profile of the film nanostructure and thickness. c) Color map describing the evolution along the ripple profile of the O/Si ratio in the films (blue color corresponds to SiO_2, red color to a SiOx´composition (x´<x), the yellow color represents a transition zone and the dark red to the Cr LIPSS structure).*

XPS analysis of the SiOx thin films deposited onto a rippled substrate

A first experimental evidence of a different film composition depending on the ripple side was obtained by angle resolved XPS analysis of samples [18,19]. For a film with a $SiO_{1.5}$ nominal composition (i.e., as obtained onto a flat substrate), the Si2p spectra obtained at different collection angles reported in Figure 4 present different shapes depending on the exit angle of photoelectrons when the sample was rotated around an axis parallel to the ripple direction (see schemes in the bottom part of the figure). Practically no changes were observed in the Si 2p spectra when the sample was rotated around an in-plane axis perpendicular to the ripple direction. Spectra in Figure 4 have been fitted under the assumption, well supported

ACCEPTED MANUSCRIPT

in previous works in literature on SiOx thin films [23-25], of the presence of five different oxidation states of silicon: Si^0, Si^+, Si^{2+}, Si^{3+}, Si^{4+}.

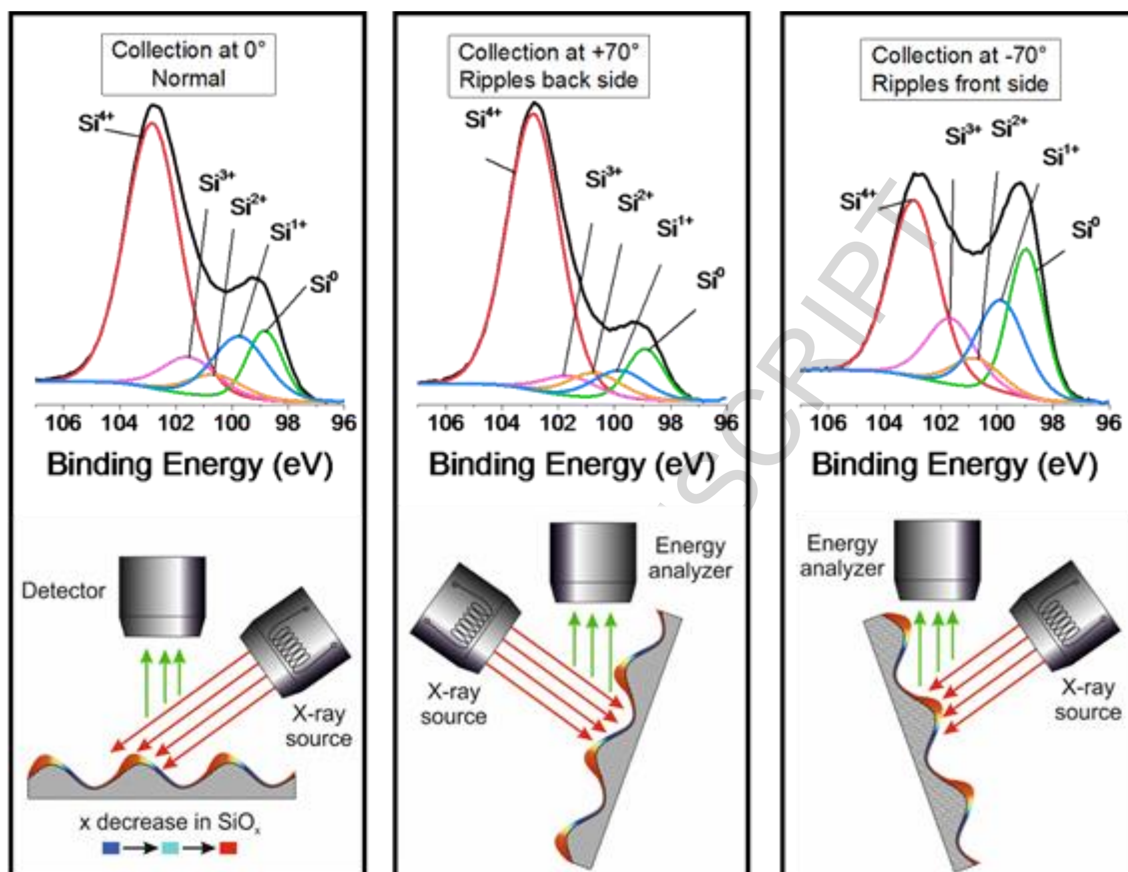

Figure 4.- Top) Fitted Si2p spectra taken for a $SiO_{1.5}$ thin film deposited on a rippled substrate for three different collection angles with respect to the substrate perpendicular (0º, +70º and -70º) of photoelectrons selected by turning the sample around an axis coinciding with the ripple direction. Fitting analysis is done with five fitting bands separated by approximately 1 eV. Bottom) Scheme of the geometrical arrangement of samples when examined by XPS with indication of photoelectron exit angles 0º, +70º and -70º defined with respect to the perpendicular to the substrate and the line of ripple direction.

The evolution in the shape of the spectra from the 0º to the +70º to the -70º photoelectron collection angles clearly demonstrate that surface composition is heterogeneous and that a depletion of oxygen (i.e., equivalent to the relative higher concentration of Si^0 and Si^+ species) occurs on the ripple side facing the particles flux during deposition. Average O/Si surface ratios of 1.48, 1.62, 1.12 were determined from the spectra taken at 0º, +70 and -70º, respectively. The percentages of the different oxidation states derived from the area of the different fitting bands at each collection angle are also reported in the supplementary

ACCEPTED MANUSCRIPT

material, (Figure S1 and Table S1) for this sample and two other examples with nominal compositions $SiO_{1.2}$ and $SiO_{1.9}$. This evolution clearly reveals that the O/Si ratio at the ripple side facing the target (x´, determined at -70º) is smaller than the average surface composition and that the O/Si ratio on the opposite side of the ripples significantly increases (x´, determined at +70º), in good agreement with the MC simulations in Figure 2 (note that a SiO_2 stoichiometry is not measured because ripples do not present a sinusoidal shape, have imperfections and at -70º photoelectrons from the top of the ripples are also collected).

AFM-Raman analysis of surface composition distribution

A microscopic assessment of the O/Si ratio distribution over the surface can be obtained by AFM-Raman analysis [20]. Figure 5 shows Raman and AFM topographic maps taken simultaneously obtained from the surface of a $SiO_{1.2}$ thin film deposited on the rippled substrate. A topographic cross sectional profile along a direction perpendicular to the ripples and the Raman spectra recorded at the blue and red zones of the Raman map are also included in this figure. Raman map reveals a preferential arrangement of the composition distribution along the direction of the LIPPS patterns and a certain 2D clustering that we attribute to the unavoidable imperfections in the LIPPS patterns (c.f. Figure 2) and some randomization along the surface of the shadowing effects that control the compositional patterning. Raman spectra of the observed zones depict shapes that are typical of SiOx films [28-30] where the features at 140, 300, 380, and 480 cm^{-1} can be associated to Si^0 species (see supplementary material, Figure S2, for a fitting analysis of these spectra according to a common attribution of the different bands in literature) and those at 606 and 630 cm^{-1} (and another broad band between 300 and 500 cm^{-1} overlapping with the Si^0 bands) to SiO2 species [31,32]. The Raman map in Figure 5 reflects the evolution of the intensity of this latter feature along the surface with the red color corresponding to those zones where it is more intense and therefore the O/Si ratio is higher. The comparison of the compositional (i.e, Raman), the topographic maps and the lineal profile in this figure clearly shows that the ripple side opposite to the flux direction of sputtered silicon species are enriched in SiO_2 which, on the contrary, becomes depleted on the other side of the ripples. We would like to note that this compositional patterning can be well controlled for certain values of the

ACCEPTED MANUSCRIPT

film thickness but progressively degrades as the film thickness increases. Experiments with SiOx thin films of 100 and 150 nm revealed a certain degradation of the composition patterning, although clear zones attributed to different compositions aligned along the direction of LIPPS were still observed. In principle, compositional patterning will remain wherever a clear topographic pattern is preserved. In a recent investigation on this question we have found that the topography of a substrate pattern affect the microstructure of thin films deposited by magnetron sputtering at oblique angles until a certain characteristic *oblivion* thickness that is in the order of the separation between pattern strips [33].

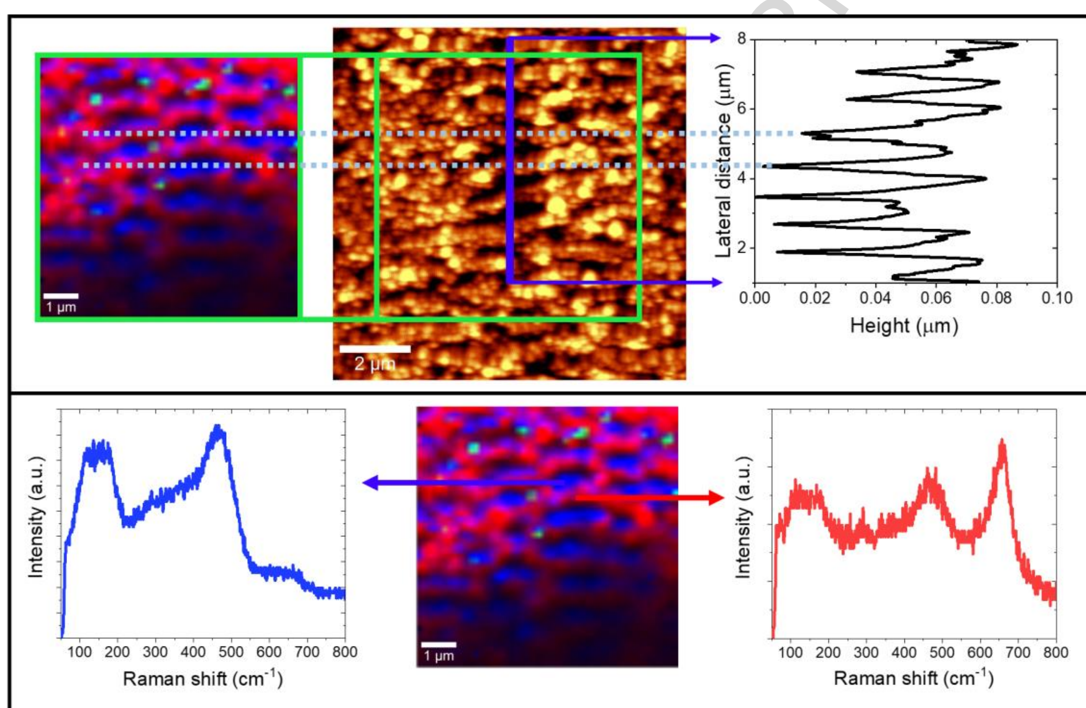

Figure 4.- AFM-Raman analysis of the $SiO_{1.2}$ thin film deposited on the ripple structure. Top) Topographic image (middle), lineal profile along the ripple direction (right) and Raman map (left). Bottom) Raman map and typical spectra recorded at the red and blue areas of the map following the band at 630 cm^{-1}.

The previous experiments clearly demonstrate that the combination of r-MS-OAD and rippled substrates is straightforward for the 2D self–patterning of thin film composition over the substrate surface. The mechanism sustaining this self-patterning process benefits from the local shadowing effects produced by the ripples during the deposition and the resulting different proportions of oxygen and silicon species arriving to the different zones of the rippled substrate. Regarding the

ACCEPTED MANUSCRIPT

former it is worth stressing that dimensions (e.g., ripple period) providing an effective control over shadowing processes and therefore composition distribution must be within hundreds of nanometers. Such a range of ripple period dimensions is within those typical of light interference phenomena or those inducing anisotropic wetting and elongated cell growth on surfaces [34, 35] and might be used for the fabrication of advanced optical devices [7,36,37] and surfaces with controlled wetting, freezing or antifouling properties [6, 38] among other possible applications. For these and other applications it is sometimes required the fabrication of substrates with a well-defined patterning of composition in order to, for example, induced specific diffractive effects, prevent the adhesion of cells or favor a one-direction sliding of liquids onto solid surfaces. The proposed methodology could be an alternative to lithographic procedures to achieve a lateral patterning of composition complying with these functionalities.

Acknowledgement

The authors thank the European Regional Development Funds program (EU-FEDER) and the MINEICO-AEI (201560E055, MAT2016-79866-R, TEC2017-82464-R projects and network MAT2015-69035-REDC) for financial support. We also acknowledge the support of the University of Seville (V and VI PPIT-US).

References

[1] S. Tawfi, M. De Volder, D. Copic, S. J. Park , C. R. Oliver, E. S. Polsen, M. J. Roberts, A. J. Hart. Engineering of micro- and nanostructured surfaces with anisotropic geometries and properties. Adv. Mater. 24 (2012) 1628-1674.

[2] Y.-M. Shin, L. R. Barnett, D. Gamzina, N. C. Luhmann Jr., M. Field, R. Borwick. Terahertz vacuum electronic circuits fabricated by UV lithographic molding and deep reactive ion etching. Appl. Phys. Lett. 95 (2009) 181505.

[3] V. R. Manfrinato, L. Zhang, D. Su, H. Duan, R. G. Hobbs, E. A. Stach, K. K. Berggren. Resolution Limits of Electron-Beam Lithography toward the Atomic Scale. Nano Lett. 13 (2013) 1555.

[4] L. Bruchhaus, P. Mazarov, L. Bischoff, J. Gierak, A.D. Wieck, H. Hovel. Comparison of technologies for nano device prototyping with a special focus on ion beams: A review. Appl. Phys. Rev. 4 (2017) 011302.

ACCEPTED MANUSCRIPT

[5] S. Ghosh, G. K. Ananthasuresh. Single-photon-multi-layer-interference lithography for high-aspect-ratio and three-dimensional SU-8 micro-/nanostructures. Scient. Rep. 6 (2016) 18428.

[6] M. J. Kreder, J. Alvarenga, P. Kim, J. Aizenberg. Design of anti-icing surfaces: smooth, textured or slippery?. Nature Rev. Mat. 1 (2016) 15003

[7] A. Di Falco, L. O'Faolain , T.F. Krauss. Chemical sensing in slotted photonic crystal heterostructure cavities. Appl. Phys. Lett . 94 (2009) 063503.

[8] N. Xiao, M.A. Villena, B. Yuan, S.C. Chen, B.R. Wang, M. Elias, Y.Y. Shi, F. Hui, X. Jing, A. Scheuermann, K.C. Tang, P.C. McIntyre, M. Lanza. Resistive Random Access Memory Cells with a Bilayer TiO2/SiOX Insulating Stack for Simultaneous Filamentary and Distributed Resistive Switching. Adv. Funct. Mater. 27 (2017) 1700384.

[9] R. Alvarez, J. M. Garcia-Martin, M. C. Lopez-Santos, V. Rico, F. J. Ferrer, J. Cotrino, A. R. Gonzalez-Elipe, A. Palmero. On the Deposition Rates of Magnetron Sputtered Thin Films at Oblique Angles. Plasma Proc. Polym. 11 (2014) 571-576.

[10] I. Gnilitskyi, V. Gruzdev, N. M. Bulgakova, T. Mocek, L. Orazi. Mechanisms of high-regularity periodic structuring of silicon surface by sub-MHz repetition rate ultrashort laser pulses. Appl. Phys. Lett. 109 (2016) 143101.

[11] J. Bonse, S. Höhm, S.V. Kirner, A. Rosenfeld, J. Krüger. Laser-Induced Periodic Surface Structures-A Scientific Evergreen. IEEE J. Select. Topics Quant. Electr. 23 (2017) 9000615.

[12] A. Barranco, A. Borras, A. R. Gonzalez-Elipe, A. Palmero. Perspectives on oblique angle deposition of thin films: From fundamentals to devices. Prog. Mat. Sci. 76 (2016) 59-153.

[13] M. Suzuki. Practical applications of thin films nanostructured by shadowing growth. J. Nanophotonic 7 (2013) 073598.

[14] G.K. Kannarpady, K.R. Khedir, H. Ishihara, J. Woo, O.D. Oshin, S. Trigwell, C. Ryerson, S. Biris. Controlled Growth of Self-Organized Hexagonal Arrays of Metallic Nanorods Using Template-Assisted Glancing Angle Deposition for Superhydrophobic Applications. ACS Appl. Mater. Interf. 3 (2011) 2332-2340.

[15] A. García-Valenzuela, R. Alvarez, C. López-Santos, F.J. Ferrer, V. Rico, E. Guillen, M. Alcon-Camas, R. Escobar-Galindo, A.R. González-Elipe, A. Palmero. Stoichiometry control of SiOx Thin films grown by reactive magnetron sputtering at oblique angles. Plasma Proc. Polym. 13 (2016)1242-1248.

[16] A. Ruiz de la Cruz, R. Lahoz, J. Siegel, G. F. de la Fuente, J. Solis. High speed inscription of uniform, large-area laser-induced periodic surface structures in Cr films using a high repetition rate fs laser. Optics lett. 39 (2014) 2491-2494.

ACCEPTED MANUSCRIPT

ACCEPTED MANUSCRIPT

[17] Y. Fuentes-Edfuf, M. Garcia-Lechuga, D. Puerto, C. Florian, A. Garcia-Leis, S. Sanchez-Cortes, J. Solis, J. Siegel. Coherent scatter-controlled phase-change grating structures in silicon using femtosecond laser pulses. Sci. Reports 7 (2017) 4594.

[18] S. Oswald M. Zier R. Reiche K. Wetzig. Angle-resolved XPS: a critical evaluation for various applications. Surf. Interf, Anal. 38 (2006) 590-594.

[19] R. A. Shircliff, P. Stradins, H. Moutinho, J. Fennell, M. L. Ghirardi, S. W. Cowley, H. M. Branz, I. T. Martin. Angle-Resolved XPS Analysis and Characterization of Mono layer and Multi layer Si lane Films for DNA Coupling to Silica. Langmuir, 29 (2013) 4057-4067.

[20] T-A. Yano, T. Ichimura, S. Kuwahara, F. H'Dhili, K. Uetsuki, Y. Okuno, P. Verma, S. Kawata. Tip-enhanced nano-Raman analytical imaging of locally induced strain distribution in carbon nanotubes. Nature Comm. 4 (2013) 2592.

[21] R. Alvarez, J.M. García-Martín, M. Macías-Montero, L. González-García, J.C. González, V. Rico, J. Perlich, J. Cotrino, A.R. González-Elipe, A. Palmero. Growth regimes of porous gold thin films deposited by magnetron sputtering at oblique incidence: from compact to columnar microstructures. Nanotechnology 24 (2013) 045604.

[22] R. Alvarez, J.M. García-Martín, A. Garcia-Valenzuela, M. Macias-Montero, F.J. Ferrer, J. Santiso, V. Rico, J. Cotrino, A.R. González-Elipe, A. Palmero. Nanostructured Ti thin films by magnetron sputtering at oblique angles. J. Phys. D: Appl. Phys. 49 (2015) 045303.

[23] A.Barranco, F. Yubero, J.P. Espinós, P. Groening, A.R. González-Elipe. Electronic state characterization of SiOx thin films prepared by evaporation. J. Appl. Physics 97 (2005) 113714.

[24] F.J. Himpsel, F.R. McFeely, A. Taleb-Ibrahimi, J.A. Yarmoff, G. Hollinger. Microscopic structure of the SiO2/Si interface. Phys. Rev. B 38 (1988) 6084-6096.

[25] A. Barranco, J.A. Mejías, J.P. Espinós, A. Caballero, A.R. González-Elipe, F. Yubero. Chemical stability of Sin+ species in SiOx (x < 2) thin films. J. Vac. Sci. Technol. A. 19 (2001)136-144.

[26] A. García-Valenzuela, R. Alvarez, V. Rico, J. Cotrino, A.R. González-Elipe, A. Palmero. Growth of nanocolumnar porous TiO2 thin films by magnetron sputtering using particle collimators. Surf. Coat. Technol. 343 (2018) 172-177.

[27] R. Alvarez, P. Romero-Gómez, J. Gil-Rostra, J. Cotrino, F. Yubero, A. Palmero, A.R. González-Elipe. On the microstructure of thin films grown by an isotropically directed deposition flux. J. Appl. Phys. 108 (2010) 064316.

[28] S. Yoo, J. Kim, B. Kang. Characterizing local structure of SiOx using confocal mu-Raman spectroscopy and its effects on electrochemical property. Electrochi. Acta 21 (2016), 68-75.

ACCEPTED MANUSCRIPT

[29] E. Baranov, S. Khmel, A. Zamchiy, M. Buyko. Structural and optical properties of a-SiOx: H thin films deposited by the GJ EBP CVD method. Phys. Stat. Sol. A 213 (2016) 1783-1789

[30] M. Klingsporn, S. Kirner, C. Villringer, D. Abou-Ras, I. Costina, M. Lehmann, B. Stannowski. Resolving the nanostructure of plasma-enhanced chemical vapor deposited nanocrystalline SiOx layers for application in solar cells. J. Appl. Phys. 119 (2016) 223104.

[31] M. Ivanda, R. Clasen, M. Hornfeck, W. Kiefer. Raman spectroscopy on SiO2 glasses sintered from nanosized particles. J. Non-Cryst. Solids 322 (2003) 46–52.

[32] P. Borowicz, M. Latek, W. Rzodkiewicz, A. Łaszcz, A. Czerwinski and J. Ratajczak. Deep-ultraviolet Raman investigation of silicon oxide: thin film on silicon substrate versus bulk material. Adv. Nat. Sci.: Nanosci. Nanotechnol. 3 (2012) 045003.

[33] A. García-Valenzuela, S. Muñoz-Piña, G. Alcalá, R. Alvarez, B. Lacroix, A.J. Santos, J. Cuevas.Maraver, V. Rico, R. Gago, L. Vázquez, J. Cotrino, A.R. González-Elipe, A. Palmero. Growth of nanocolumnar Thin films on patterned substrates at oblqieu angles. Plasma Process Polym. 16 (2019) e1800135 1-10.

[34] E. Rebollar, I. Frischauf, M. Olbrich, T. Peterbauer, S. Hering, J. Preiner, P. Hinterdorfer, C. Romanin, J. Heitz. Proliferation of aligned mammalian cells on laser-nanostructured polystyrene. Biomaterials 29 (2008)1796-1806.

[35] E. Martinez, E. Engel, J.A. Planell, J. Samitier. Effects of artificial micro- and nano-structured surfaces on cell behavior. Annals Anat. 191 (2009) 126-135.

[36] Z. Bisadi, M.Mancinelli, S.Manna, S. Tondini,M. Bernard, A. Samusenko, M. Ghulinyan, G. Fontana, P. Bettotti, F. Ramiro-Manzano, G. Pucker, L. Pavesi. Silicon nanocrystals for nonlinear communication. Phys. Status Solidi A 212 (2015) 2659-2671.

[37] L. Shi, J. T. Harris, R. Fenollosa, I. Rodriguez, X. Lu, B. A. Korgel, and F. Meseguer. Monodisperse silicon nanocavities and photonic crystals with magnetic response in the optical region. Nature Comm. 4 (2013) 1904

[38] L. Mishchenko, M. Khan, J. Aizenberg, B. D. Hatton. Spatial Control of Condensation and Freezing on Superhydrophobic Surfaces with Hydrophilic Patches. Adv. Funct. Mater. 23 (2013) 4577-4584.

ACCEPTED MANUSCRIPT

Graphical abstract

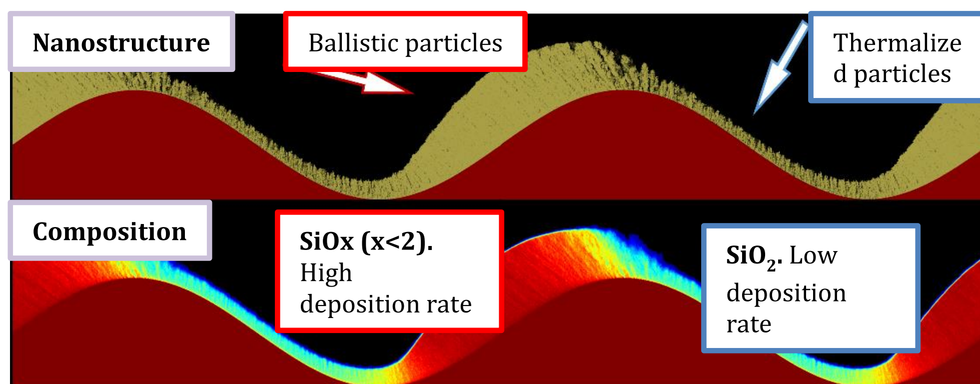

ACCEPTED MANUSCRIPT

ACCEPTED MANUSCRIPT

2D compositional self-patterning in magnetron sputtered thin films

Aurelio García-Valenzuela,[1] Rafael Alvarez,[1,2] Victor Rico,[1] Juan P. Espinos,[1] Maria C. López-Santos,[1] Javier Solís,[3] Jan Siegel,[3] Adolfo del Campo,[4] Alberto Palmero,[1] Agustín R. González-Elipe[1*]*

HIGHLIGTS

1.-Lateral patterning of thin film composition can be achieved by controlling the deposition conditions during reactive magnetron sputtering

2.- LIPPS structures are used as substrates for inducing the self-patterning of composition in length scales of the order of hundreds nanometers

3.-SiOx thin films with laterally variable composition (i.e. different O/Si ratio) have been prepared by the proposed methodology

4.-Angle resolved XPS and AFM-Raman analysis have proved the lateral distribution of composition in the prepared films

5.-Monte Carlo simulations serve to account for the basic processes intervening in the plasma gas and that are responsible for the compositional patterning

ACCEPTED MANUSCRIPT